Hydrogen/Air Combustion Calculations: The Chemical Basis of Efficiency in Hypersonic Flows

David M. Harradine,* John L. Lyman,† Richard C. Oldenborg,‡ Garry L. Schott,§
and Harry H. Watanabe¶
Los Alamos National Laboratory, Los Alamos, New Mexico 87545

The combustion of premixed hydrogen and air is investigated under conditions relevant to scramjet propulsion. A comprehensive hydrogen/air kinetics mechanism is used that suffices to model combustion in air, including HO_2 and H_2O_2 chemistry but excluding carbon compounds. The primary objective is to understand the chemical inefficiencies of combustion in hypersonic flows. In this regard, the chemistry in streamlines within a hypothetical hypersonic combustor is investigated. Computational results based on equilibrium assumptions and finite-rate kinetics are compared. A sensitivity analysis identifies three-body recombination steps to be the rate-limiting chemical reaction pathways. The effects of different nozzle profiles and of compression ratios on the chemistry are also examined. Low-density air poses an obstacle to completion of combustion in scramjets because H_2O is thermodynamically not stable enough against dissociation when combustor temperatures become too high. A significant fraction of the combustion may require completion during expansion by the three-body recombination of molecular fragments. Compositional freezing thus sacrifices a potentially greater fraction of the ideal combustion energy than in systems whose plenum gases are significantly more dense.

I. Introduction

COMPARED with the more conventional subsonic or supersonic combustion processes, hypersonic combustion offers intriguing challenges. These challenges involve tradeoffs between the aerodynamic constraints imposed by high-Mach-number flight and the desire to construct the most efficient scramjet engine possible. High-Mach-number flight requires that the scramjet propulsion system operate at low static pressures and high internal velocities. As a result, the burning fuel has very short residence times (milliseconds) in the hypersonic engine. By contrast, most conventional engines have fairly long residence times, and operate at relatively high pressures, where both propagation (bimolecular) and recombination (termolecular) reactions are fast. The low-pressure regime where the hypersonic engine operates, will slow these reaction rates, particularly the recombination of reaction intermediates, which may limit combustion efficiency. The high temperatures encountered as a result of the burn will also limit the combustion efficiency by restricting the extent of product formation by the recombination process. Thus, reaction kinetics play a much more important role than in conventional engines. More emphasis needs to be placed on the rates of the chemical reactions and on the consequent release of translational energy in the comprehensive combustion simulation codes currently used to model hypersonic combustion. We have engaged in a modeling effort to examine hypersonic combustion processes to determine the chemical causes of inefficiencies in scramjet engines.

II. Code Description

Computations were performed using a chemical kinetics code originally developed at Los Alamos to model homogeneous gas phase chemical reactions. It uses a simultaneous differential equation solver that is appropriate for "stiff" sets of differential equations. The code solves all the differential rate equations that describe the chemical reactions in combustion based on a complete reaction mechanism for hypersonic engines. No simplifying assumptions are made concerning the attainment of partial equilibria.

Modifications were made to the basic kinetics code to allow for area changes and expansion cooling in both the combustor and nozzle. The expansion was incorporated into the code as quasi-one-dimensional flow with heat addition from chemistry. It was derived from three conservation equations in mass (1), momentum (2), and energy (3), and the equation of state (4),

$$\frac{d\rho}{\rho} + \frac{dv}{v} + \frac{dA}{A} = 0 \tag{1}$$

$$v\,dv = -\frac{dP}{\rho} \tag{2}$$

$$dq = dH - \frac{1}{\rho}dP \tag{3}$$

*Staff Member, Photochemistry and Photophysics Group, Chemical and Laser Sciences Division.

†Laboratory Fellow, Photochemistry and Photophysics Group, Chemical and Laser Sciences Division.

‡Deputy Group Leader, Photochemistry and Photophysics Group, Chemical and Laser Sciences Division.

§Staff Member, Reaction Science Group, Dynamic Testing Division.

¶Group Leader, Process Development Group, Chemical and Laser Sciences Division.

$$\frac{dP}{P} = \frac{d\rho}{\rho} - \frac{dm}{m} + \frac{dT}{T} \qquad (4)$$

where ρ is the mass density, v the velocity, A the cross-sectional area of the combustor or nozzle, P the pressure, H the enthalpy, dq the difference between final and initial energies as a result of chemical change at fixed temperature, and m the average molecular weight.

The chemical rate computations included thermochemical information and integrated the evolution over time of the gas composition and accompanying thermodynamic state. Heat capacities were calculated using a statistical thermodynamic formalism with a temperature-dependent vibrational partition function and the known vibrational frequencies of the individual reactive species. A rigid-rotor, harmonic oscillator approximation was assumed.

A key index for interpretation is the energy yield, or completeness, of combustion at an intermediate or exit station of the combustor and/or nozzle. This is defined as the fraction (Q_h) of the ideal enthalpy of reaction. The initial gas mixture consists of only H_2, O_2, and N_2, whose enthalpies of formation are all zero. Thus, only final-state terms appear in the energy yield expression

$$Q_h = \sum_i \frac{f_i H_i}{y_{H_2O} H_{H_2O}} \qquad (5)$$

The index i in the numerator includes all the product species produced with a mole fraction f_i and with a molar enthalpy of formation H_i. The final product in an ideal reaction is just water and, for nonstoichiometric mixtures, residual reactants. The only nonzero term in the denominator is for H_2O; its ideal yield is denoted y_{H_2O}.

Calculations were started at the fuel inlet of the combustor. The assumptions of instantaneous mixing and noninteracting

streamlines (no diffusion, convection, or conduction) were made, and the chemistry was not allowed to alter the upstream flow pattern. Our purpose was to understand qualitatively the role chemistry plays in a hypersonic engine, rather than to obtain quantitative predictions of actual scramjet performance. Our calculations in the combustor represent only a limiting case of a realistic hypersonic engine because turbulent mixing and other factors may strongly influence the chemistry in this region. However, these calculations should be more nearly representative of actual nozzle performance. To model a realistic engine at particular Mach numbers, we took approximate starting conditions from cases tabulated by Billig.[1]

Air entering the intake undergoes compression to higher pressures and temperatures. This compression is not a gradual process but rather includes one or more abrupt increases at shock boundaries. Compression increases the internal energy of the air mixture which, in turn, causes some molecular dissociation of species such as oxygen. It is important to quantify the creation of atomic oxygen because it shortens the fuel ignition time. The air mixture is not at equilibrium at the fuel injection point. The initial starting conditions for our calculations do not examine the chemistry of the inlet and, thus, will not quantitatively calculate ignition times. Ignition, however, is probably not an issue at higher Mach numbers because of the high inlet temperature. At lower Mach numbers ($M < 8$), ignition delay may play a more significant role in determining overall performance.

At selected steps in the combustor, a sensitivity analysis was performed that determined which reactions were making predominant effects on energy yield, thus identifying the key rate-limit element per step and to what extent the combustion was tracking equilibrium conditions. The effects on combustion efficiencies of changing pressure and temperature in the combustion region, implemented through changes in contraction ratio, different area expansions in the nozzle to control temperature, and fuel-to-air ratios, were examined in order to help identify conditions for maximizing chemical yield.

Table 1 Elementary reactions for modeling prompt combustion of hydrogen in gasdynamically heated air

Reactants	Products	A, molecular units	Ea, Kcal	n	Forward rate source	$K_{eq} = k_f/k_r$, function or source
1. $H_2 + OH$	$\leftrightarrow$ $H + H_2O$	1.66×10^{-16}	3.300	1.60	2	5
2. $O_2 + H$	$\leftrightarrow$ $O + OH$	1.99×10^{-07}	16.515	−0.91	2	5
3. $H_2 + O$	$\leftrightarrow$ $H + OH$	2.49×10^{-17}	7.553	2.00	2	5
4. $H_2O + O$	$\leftrightarrow$ $OH + OH$	2.49×10^{-14}	17.260	1.14	2	K_3/K_1
5. $H + H(+H_2)$	$\leftrightarrow$ $H_2(+H_2)$	2.68×10^{-31}	0.000	−0.60	2	5
	$k_{N_2}/k_{H_2} = 0.5$ $k_{H_2O}/k_{H_2} = 5^c$					
6. $H + OH(+H_2O)$	$\leftrightarrow$ $H_2O(+H_2O)$	3.86×10^{-25}	0.000	−2.00	2	$K_1 K_5$
	$k_{N_2}/k_{H_2O} = 0.2$ $K_{H_2}/k_{H_2O} = 0.2^c$					
7. $O_2 + H(+H_2)$	$\leftrightarrow$ $HO_2(+H_2)$	5.52×10^{-30}	0.000	−0.80	2	7
	$k_{N_2}/k_{H_2} = 0.43$ $k_{H_2O}/k_{H_2} = 6.7^c$					
8. $H + O(+N_2)$	$\leftrightarrow$ $OH(+N_2)$	1.66×10^{-31}	−0.600	0.00	8	a
	$k_{N_2}/k_{H_2} = 0.4$ $k_{H_2O}/k_{H_2} = 6.5^c$					
9. $H + HO_2$	$\leftrightarrow$ $OH + OH$	4.15×10^{-10}	1.888	0.00	10	$K_2 K_3(K_5/K_7)$
10. $O + HO_2$	$\leftrightarrow$ $OH + O_2$	3.32×10^{-11}	0.000	0.00	2	$K_3(K_5/K_7)$
11. $OH + HO_2$	$\leftrightarrow$ $H_2O + O_2$	3.32×10^{-11}	0.000	0.00	2	$K_1(K_5/K_7)$
12. $H + HO_2$	$\leftrightarrow$ $H_2 + O_2$	4.15×10^{-11}	0.693	0.00	2	K_5/K_7
13. $OH + H_2O_2$	$\leftrightarrow$ $H_2O + HO_2$	1.16×10^{-11}	1.430	0.00	2	a
14. $O + H_2O_2$	$\leftrightarrow$ $OH + HO_2$	1.60×10^{-17}	3.970	2.00	9	a
15. $H + H_2O_2$	$\leftrightarrow$ $H_2 + HO_2$	2.82×10^{-12}	3.752	0.00	2	2
16. $H + H_2O_2$	$\leftrightarrow$ $H_2O + OH$	1.66×10^{-11}	3.580	0.00	2	a
17. $HO_2 + HO_2$	$\leftrightarrow$ $O_2 + H_2O_2$	3.32×10^{-12}	0.000	0.00	2	a
18. $H_2O_2(+N_2)$	$\leftrightarrow$ $OH + OH(+N_2)$	2.00×10^{-07}	45.500	0.00	2	a
	$k_{N_2}/k_{H_2} = 0.4$ $k_{H_2O}/k_{H_2} = 6.5^c$					
19. $O + NO$	$\leftrightarrow$ $N + O_2$	6.32×10^{-15}	41.370	1.00	3	b
20. $O + N_2$	$\leftrightarrow$ $NO + N$	3.02×10^{-10}	76.241	0.00	3	b
21. $H + NO$	$\leftrightarrow$ $N + OH$	4.37×10^{-10}	50.410	0.00	3	$K_2 K_{19}$
22. $O + O(+O_2)$	$\leftrightarrow$ $O_2(+O_2)$	2.76×10^{-33}	0.000	0.00	4	$K_2/(K_3 K_5)$
	$k_{N_2}/k_{O_2} = 0.3$					

^{a}The equilibrium constant was derived using room temperature entropies and enthalpies from JANAF tables.
^{b}The equilibrium constant was estimated as the quotient of the recommended forward and reverse rate expressions from Ref. 6.
^{c}Collision efficiencies for reactions 5 and 6 estimated from Ref. 10, reaction 7 from Ref. 7, and reactions 8 and 18 from Ref. 2.

III. Hydrogen/Air Reaction Mechanism

The reaction mechanism adopted as input to the kinetics code used elementary reaction steps and their rate coefficients obtained from published sources[2-10]; these elementary reactions are assembled in Table 1. This mechanism was scoped to treat compositions with either fuel or air in excess, as well as near-stoichiometric ones, and to deal with reaction times from about 10^{-5} to 10^{-2} s and static gas temperatures reached adiabatically in gas-dynamically compressed or expanded flows. Besides the oxidation of hydrogen, reversible chemical conversion of atmospheric N_2 to NO was included. Most recently, the chemistry of hydrogen peroxide combustion was incorporated into our mechanism, because of concerns in the combustion community that its role may cause significant shifts in the energy release outcome. We have determined that these fears are unfounded. The eleven individual species involved in one or more reactions are: H_2, O_2, H_2O, H_2O_2, OH, H, O, HO_2, N_2, NO, and N. For each of the 22 reaction steps listed in Table 1, the forward sense is indicated by the left-to-right arrow, and the net rate is the difference, $R_{net} = (R_f - R_r)$, between individual forward and reverse rates, R_f and R_r, respectively. The coefficients that multiply the corresponding concentrations in these terms are k_f and k_r, and each is represented as a function of absolute temperature T by

$$k = AT^n \exp(-E_a/RT) \qquad (6)$$

The set (A, n, E_a) for k_f has been taken from the source indicated in column 6 of Table 1. In order that each R_{net} vanish at equilibrium, k_r is derived as $k_r = k_f/K_{eq}$, where K_{eq} is the ideal-gas thermodynamic equilibrium constant. Within Table 1, an available set of independent K_{eq} functions was compiled from the literature sources for reactions 1, 2, 3, 5, 7, 18, 19, and 20; the others were derived from those reactions as indicated.
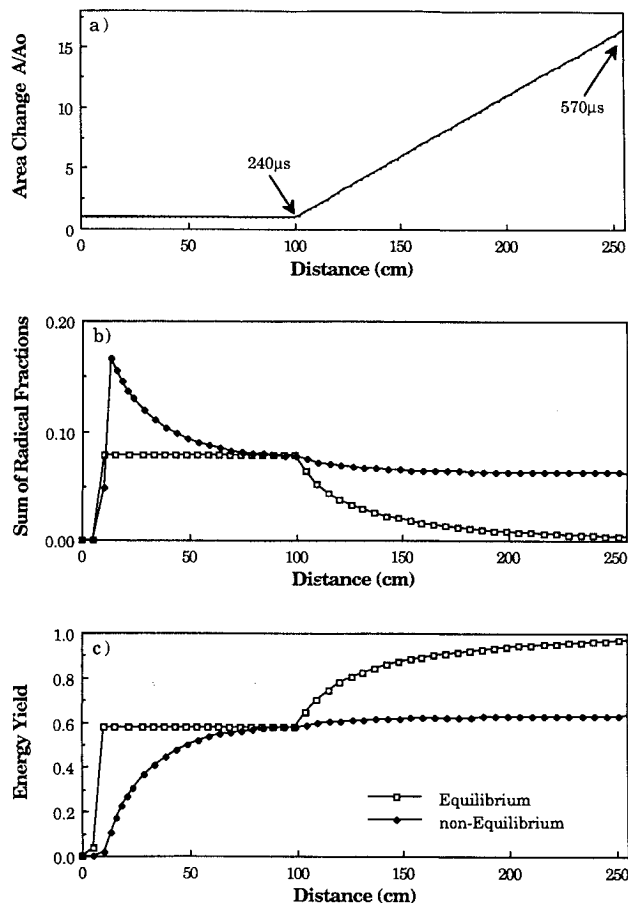
IV. Results and Discussion

Combustion calculations were performed at several flow conditions. This paper shows only the results obtained for a Mach 15 case. The approximate initial starting temperatures, pressures, and velocities were obtained from Ref. 1 and are shown in Table 2, along with corresponding starting densities.

Equilibrium vs Finite-Rate Chemistry

The first calculations performed were to examine the differences between combustors constrained to maintain equilibrium and combustors with the full finite-rate chemistry included. The equilbrium calculations (the open squares of Figs. 1b and 1c) were obtained by increasing the individual rates of a subset of the whole mechanism to a point at which the kinetics were no longer the limiting factor. Both calculations were for a stoichiometric mixture of hydrogen and air. Figure 1a shows the profile of a model hypersonic engine. The combustor was straight-walled to 100 cm. The nozzle slope for all calculations, except where noted, was $\partial A'/\partial x = 0.1$ cm^{-1}, where x is the distance traveled and A' the ratio of the area to the initial area, A/A_0.

A plot of the sum of all radicals species (H, O, OH, HO_2, N, NO) relative to the total density is presented in Fig. 1b. It is seen that the radical fractions in the finite-rate chemistry case far overshoot their equilibrium populations following ignition, as generally observed in the behavior of hydrogen/oxygen plug flow.[11] Recombination via termolecular reactions brings the total radical chemistry down to its equilbrium state just before the end of the combustor. During this time, the temperature has risen from the initial 1463 K to 2932 K. This high temperature limits the maximum possible energy yield attainable to 58% at the end of the combustor. At higher Mach numbers, we find that the decreased residence time in the combustor, coupled with lower species densities, does not allow the achievement of equilibrium by the 100-cm point whereas, at lower Mach number, equilibrium is more easily obtained.

In the nozzle region, very little additional recombination takes place before the mixture becomes kinetically frozen and ceases to follow equilibrium. The resultant chemical efficiency or energy yield is presented in Fig. 1c. The difference between the net heat release of the equilibrium constrained case and the kinetics limited case is extreme, and it is even more pronounced at higher Mach number. The effect of finite-rate dissociation-recombination chemistry is to lower the energy yield below that expected for equilibrium chemistry. It is clear that nonequilibrium chemistry plays a significant role in high-Mach-number scramjets compared to a more conventional engine where the chemistry is fast enough to maintain equilibrium.

Sensitivity Analysis

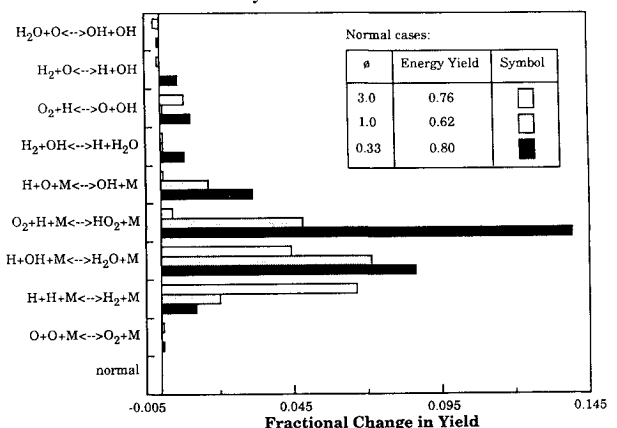Comparing a sensitivity analysis, such as that presented, with the current accuracy to which the individual rates of the

Fig. 1   Equilibrium vs finite-rate kinetics for a stoichiometric fuel/air mixture.

Fig. 2   Sensitivity of energy yield at nozzle end to reaction rates; ϕ is the equivalence ratio.
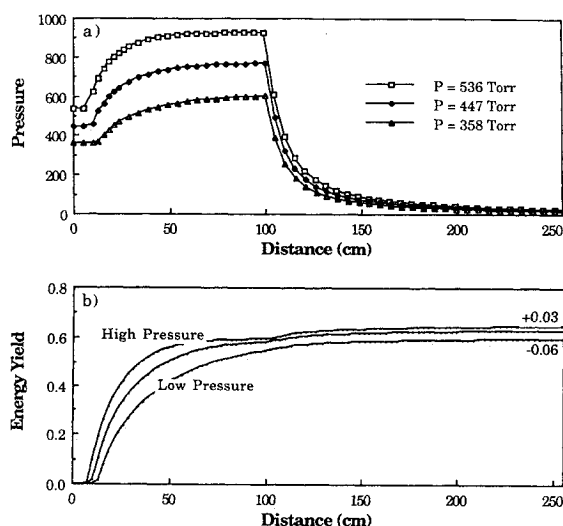
Fig. 3 Effects on energy release with 20% changes in pressure at 1463 K inlet temperature.

Fig. 4 Effects on energy release with 20% variations in temperature at 447-Torr inlet pressure.

H_2/air combustion mechanism are known determines which steps introduce the greatest uncertainties in this simulation. Figure 2 shows this analysis for five of the recombination reactions and four of the important ignition and chain branching steps included in our mechanism. The bars on this graph represent a fractional change in the yield at the end of the nozzle after the individual reaction rate constant and its corresponding reverse reaction were multiplied by a factor of 5.[2] The results indicate that it is the three-body recombination reactions that determine the amount of heat release. The four other reactions shown in Fig. 2 are the bimolecular reactions that exhibit the greatest sensitivity in the determination of the heat release. The chemistry involving HO_2 and H_2O_2 (Table 1, reactions 9–18) was also examined (not shown in Fig. 2), but changes in the rates of this chemistry had virtually no effect on the outcome. Two-body reactions are believed to be of more importance in the ignition sequence,[8] which was not examined in detail for this paper. Since ignition is fast under these conditions, the two-body reactions involved in the ignition sequence are important only at the beginning. Thus, uncertainties in these reaction rates play little role in nozzle exit efficiencies. Reactions 9–12 are, however, an essential link in the recombination through reaction 7, which involves HO_2. These rates are so fast already that the factor of 5 increase makes little additional difference.

The influence of the recombination reactions 5–8 on the yield occurs principally in the early stages of nozzle expansion before the reaction mixture freezes out. Of the termolecular reactions, only the reverse of reactions 18 and 22 are slow enough so that increasing their rates makes no appreciable difference to energy yield. A similar analysis was done at a midcombustor point ($x = 50$ cm), well after ignition but before the system was in complete equilibrium. The effects of higher rates of the key reactions are qualitatively similar at this point to those displayed in Fig. 2, except that the fractional change in the energy yield is up to a factor of 5 larger.

The effect of equivalence ratio on energy yield sensitivities to rate constant changes is also shown in Fig. 2. Sets of calculations were produced for the Mach 15 case at three fuel mixture ratios; $\phi = 0.33$, 1.0, and 3.0 (see Table 2). Although the termolecular reactions are always the most important set of reactions, the relative importance of each termolecular reaction changes from fuel-lean to fuel-rich conditions. The $H + H + M$ recombination reactions dominate in fuel-rich conditions, where a factor of 5 increase produces a 7% increase in energy yield, whereas $O_2 + H + M$ predominates under the fuel-lean condition (almost a 15% increase). The $H + OH + M$ reactions are important in all mixtures and, unfortunately, probably have the least well-known rate constants.
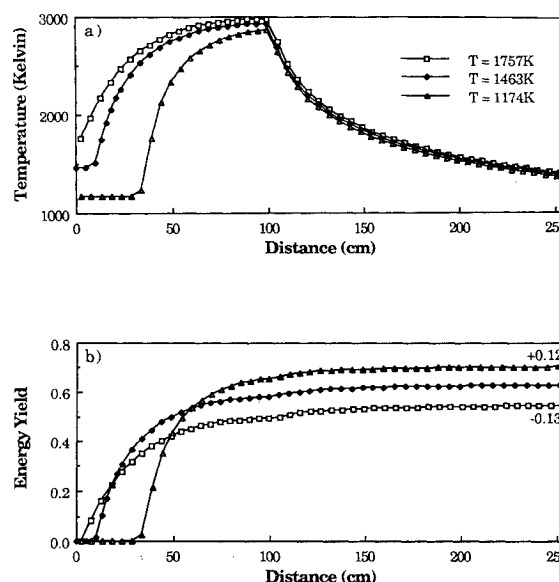
Table 2 Initial combustor inlet conditions for a freestream Mach 15 case;

temperature = 1463 K		pressure = 434 Torr		velocity = 434,093 cm/s[a]
ϕ	H_2[b]	O_2[b]	N_2[b]	Ar[b]
0.33	3.619×10^{17}	5.428×10^{17}	2.024×10^{18}	2.516×10^{16}
1.00	8.719×10^{17}	4.360×10^{17}	1.625×10^{18}	1.996×10^{16}
3.00	1.644×10^{18}	2.741×10^{17}	1.022×10^{18}	1.270×10^{16}

[a]Velocity is with respect to the combustor.
[b]In units of molecules/cc.

Effects of Changing Compression Ratios

Changing the compression ratio of the air to the combustor can affect the chemistry in the hypersonic engine by altering the temperature, gas, density, and the velocity of the gas flow. To obtain an intuitive feel for what may happen to the chemistry and, subsequently, the energy output, the initial temperature and pressure were systematically varied at the combustor inlet. These results are presented in Fig. 3 and 4.

In Fig. 3a, the initial starting pressure was varied ±20% from the value stated in Table 2 by changing the initial starting species densities (a unity equivalence ratio was maintained) and keeping the starting temperatures constant. The energy yield shown in Fig. 3b, as expected, is highest at higher pressures because of increased recombination rates. However, the percent change from the base case at nozzle end was only +3% and −6%. In Fig. 4, the effect of changing the initial temperature by ±20% is examined. The initial pressure was kept constant by allowing the species density to change in accordance with the temperature change. This scenario approximates the effects of changing contraction ratios, in agreement with Ref. 1. The most obvious effect of changing temperatures is to alter dramatically the relative ignition times; in the low-temperature case, equilibrium is not even achieved by combustor end. Despite this, the lowest-temperature case produces the highest yield (Fig. 4b). The lower temperature is accompanied by higher density, both of which favor recombination, first, by shifting equilibrium toward products and, second, by an increase in collision rate. The effects of changing temperature cannot be completely decoupled from pressure or density changes, but it is apparent that an inlet designed to produce higher densities with lower temperatures, perhaps by cold-fuel injection, will produce a more efficient engine. This analysis examines only scramjet performance and does not
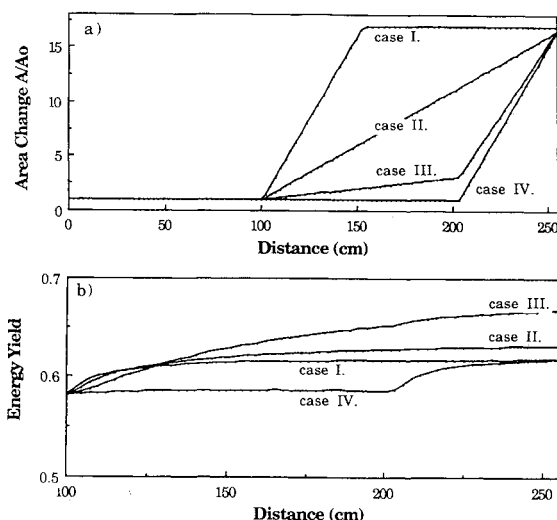
Fig. 5   Variations in energy yield for different nozzle contours.

consider the effect these changes will have on vehicle drag and overall performance.

Changes in Nozzle Contours

As a final point of analysis, the effects of different nozzle contours on heat release were compared. Figure 5a depicts the different profiles used for this comparison. Case I started with a rapid flare-out at the beginning of the nozzle and was then straight-walled to the end of the calculation. Case II had a simple linear expansion rate and is the base case to all previous calculations shown. In case III, the nozzle started with a slight expansion and flared quickly to the end, an approximation of a horn-shaped nozzle. Finally, case IV essentially extended the combustor until it again quickly flared out at the same rate as in case I to the finish of the calculation. All shapes came to the same A/A_0 point (≈ 17), so that the only effect on chemistry was one of changing paths, not overall area expansion. The energy-yield axis shown in Fig. 5b has been expanded to encompass just the nozzle region. The best heat release is provided by case III. The small expansion rate ($dA'/dx = 0.02$ cm^{-1}) at the beginning of the nozzle allows the chemistry to track equilibrium to a larger expansion before freezing out. This case eventually produces 8% more energy at nozzle end vs case I or IV. In the other three cases, the beneficial effects that decreasing temperature has on shifting equilibrium toward products (i.e., decreasing the radical fragments) are quickly overcome by a rapid drop in pressure. Because differences in energy yield will result in changes in the terminal exit velocity, careful attention to nozzle contour can play an important role in attaining the maximum possible thrust.

V. Summary and Conclusions

From the results of the study, several conclusions can be drawn as to the effect chemistry will have on the efficient utilization of atmospheric oxygen in a hypersonic combustor:

1) A realistic code must incorporate finite-rate chemistry in order to account properly for chemical energy yield at the termination of the hypersonic engine, i.e., equilibrium cannot be assumed.

2) The most critical class of reactions in terms of limiting the maximum heat release are the three-body termolecular reactions (Table 1, reactions 5-7). This influence results primarily from the low operating pressures in the hypersonic engine and is relatively independent of equivalence ratio. The problem manifests itself with the possibility of never reaching equilibrium in the combustor and with frozen expansions in the nozzle. Since this class of reactions is the most important, any uncertainty in these rate constants will introduce the greatest error in performance simulations.

3) H_2O_2 chemistry (reactions 13-18) is not important under conditions at high Mach number. In high-temperature combustion, these processes are probably not important. At the lowest Mach numbers, when the initial temperature is lower, their participation may become of more concern, particularly with regard to ignition.

4) Changes in inlet design that increase density and decrease temperature will enhance scramjet energy yield. However, the effect of these design changes on vehicle drag and overall performance cannot be deduced from the simple analysis presented here.

5) The design of the nozzle contour will play a significant role in the amount of chemical energy that can be released. This is again a question of frozen expansion vs equilibrium expansion. Slight expansion in the transition from the combustor to the nozzle before a rapid expansion may be desirable to cool high exhaust temperatures while maintaining equilibrium and promoting product formation. A high radical concentration at the nozzle exit is the direct cause of decreased energy extraction.

Low-density air poses a fundamental obstacle to completion of combustion in scramjets because H_2O and any excess H_2 or O_2 are thermodynamically unstable when temperatures become too high before expansion. This instability can leave a significant fraction of the combustion to be accomplished during expansion by three-body recombination of molecular fragments. In our base case, stoichiometric mixture example for Mach 15 flight, this fraction represented 41% of the ideal enthalpy of reaction. In scramjets, the combination of high axial speed and progressively reduced gas density through the expansion readily causes kinetic freezing of the gas composition, with sacrifice of a macroscopic fraction of the theoretical combustion energy. This fraction is potentially much larger than is typical in rockets,[12] where plenum gases are somewhat hotter but >20 times more dense.

References

[1]Billig, F. S., "Combustion Processes in Supersonic Flow," *Journal of Propulsion and Power*, Vol. 4, May-June 1988, pp. 209-216.

[2]Gardiner, W. C., Jr. (ed.), *Combustion Chemistry*, Springer-Verlag, NY, 1984, pp. 204-227.

[3]Gardiner, W. C., Jr. (ed.), *Combustion Chemistry*, Springer-Verlag, NY, 1984, pp. 361-421.

[4]Baulch, D. L., Drysdale, D. D., Duxbury, J., and Grant, S., *Evaluated Kinetic Data for High Temperature Reactions*, Vol. III, *Homogeneous Gas Phase Reactions of the O_2-O_3 System, CO-CO$_2$-H_2 System, and of Sulphur-Containing Species*, Butterworths, London, 1976.

[5]Cohen, N., and Westberg K., "Chemical Kinetic Data for High-Temperature Reactions," *Journal of Physical and Chemical Reference Data*, Vol. 12, 1983, pp. 551-562.

[6]Baulch, D. L., Drysdale, D. D., and Horne, D. G., *Evaluated Kinetic Data for High Temperature Reactions*, Vol. II, *Homogeneous Gas Phase Reactions of the H_2-N_2-O_2 System*, Butterworths, London, 1973.

[7]Dixon-Lewis, G., "Spherically Symmetric Flame Propagation in Hydrogen Air Mixtures," *Combustion Science and Technology*, Vol. 34, 1983, pp. 1-29.

[8]Jachimowski, C. J., "An Analytical Study of the Hydrogen-Air Reaction Mechanism with Application to Scramjet Combustion," NASA TR-2791, Feb. 1988.

[9]Tsang, W., and Hampson, R. F., "Chemical Kinetic Data Base for Combustion Chemistry. Part I. Methane and Related Compounds," *Journal of Physical and Chemical Reference Data*, Vol. 15, 1986, pp. 1087-1279.

[10]Baulch, D. L., Drysdale, D. D., Horne, D. G., and Lloyd, A. C., *Evaluated Kinetic Data for High Temperature Reactions*, Vol. I, *Homogeneous Gas Phase Reactions of the H_2-O_2 Systems*, Butterworths, London, 1972.

[11]Schott, G. L., "Kinetic Studies of Hydroxyl Radicals in Shock Waves. III. The OH Concentration Maximum in the Hydrogen-Oxygen Reaction," *Journal of Chemical Physics*, Vol. 32, 1960, p. 710.

[12]Matsuzaki, R., Hirabayashi, N., and Tanaka, T., "Gas Dynamic Properties of an Oxygen-Hydrogen Engine Nozzle at Extremely High Pressures," AIAA Paper 88-2717, June 1988.